

## MYELOID NEOPLASIA

## Alternative polyadenylation dysregulation contributes to the differentiation block of acute myeloid leukemia

Amanda G. Davis,<sup>1,2</sup> Daniel T. Johnson,<sup>1,2</sup> Dinghai Zheng,<sup>3</sup> Ruijia Wang,<sup>3</sup> Nathan D. Jayne,<sup>1,2</sup> Mengdan Liu,<sup>1,2</sup> Jihae Shin,<sup>3</sup> Luyang Wang,<sup>4</sup> Samuel A. Stoner,<sup>1</sup> Jie-Hua Zhou,<sup>5</sup> Edward D. Ball,<sup>5</sup> Bin Tian,<sup>3,4</sup> and Dong-Er Zhang<sup>1,2,6</sup>

<sup>1</sup>Moore's Cancer Center and <sup>2</sup>Division of Biological Sciences, University of California San Diego, La Jolla, CA; <sup>3</sup>Department of Microbiology, Biochemistry, and Molecular Genetics, Rutgers New Jersey Medical School, Newark, NJ; <sup>4</sup>Program in Gene Expression and Regulation, Center for Systems and Computational Biology, The Wistar Institute, Philadelphia, PA; <sup>5</sup>Division of Blood and Marrow Transplantation, Department of Medicine; and <sup>6</sup>Department of Pathology, University of California San Diego, La Jolla, CA

## KEY POINTS

- FIP1L1 knockdown reverses global APA dysregulation in t(8;21) AML and promotes differentiation by 3'UTR lengthening of AML1-ETO.
- Targeting APA induces differentiation across AML subtypes by downregulation of MYC and attenuation of oncogenic growth signaling pathways.

Posttranscriptional regulation has emerged as a driver for leukemia development and an avenue for therapeutic targeting. Among posttranscriptional processes, alternative polyadenylation (APA) is globally dysregulated across cancer types. However, limited studies have focused on the prevalence and role of APA in myeloid leukemia. Furthermore, it is poorly understood how altered poly(A) site usage of individual genes contributes to malignancy or whether targeting global APA patterns might alter oncogenic potential. In this study, we examined global APA dysregulation in patients with acute myeloid leukemia (AML) by performing 3' region extraction and deep sequencing (3'READS) on a subset of AML patient samples along with healthy hematopoietic stem and progenitor cells (HSPCs) and by analyzing publicly available data from a broad AML patient cohort. We show that patient cells exhibit global 3' untranslated region (UTR) shortening and coding sequence lengthening due to differences in poly(A) site (PAS) usage. Among APA regulators, expression of *FIP1L1*, one of the core cleavage and polyadenylation factors, correlated with the degree of APA dysregulation in our 3'READS data set. Targeting global APA by FIP1L1 knockdown reversed the global trends seen in patients. Importantly, FIP1L1 knockdown induced differentiation of t(8;21) cells by promoting 3'UTR lengthening and downregulation of the fusion oncoprotein AML1-ETO.

In non-t(8;21) cells, FIP1L1 knockdown also promoted differentiation by attenuating mechanistic target of rapamycin complex 1 (mTORC1) signaling and reducing MYC protein levels. Our study provides mechanistic insights into the role of APA in AML pathogenesis and indicates that targeting global APA patterns can overcome the differentiation block in patients with AML.

## Introduction

Posttranscriptional regulation is an emerging field of study in normal and malignant hematopoiesis.<sup>1</sup> Among posttranscriptional processes, splicing regulation has been the predominant focus, owing to the high instance of splice factor mutations across hematologic malignancies.<sup>2</sup> In addition, RNA-editing,<sup>3</sup> RNA-methylation,<sup>4</sup> and microRNA (miRNA) regulation<sup>5</sup> have been linked to proper hematopoietic stem cell (HSC) homeostasis. Despite the importance of posttranscriptional regulation in hematopoietic systems, there has been comparatively little attention paid to the process of alternative polyadenylation (APA), and studies have exclusively focused on APA in lymphocytes.<sup>6-12</sup> Furthermore, it is unknown whether polyadenylation regulators contribute to myeloid cell development or myeloid leukemia.

APA is a widespread posttranscriptional mechanism, with the potential to regulate most human genes.<sup>13</sup> Differences in poly(A) site (PAS) usage in the 3' untranslated region (3'UTR), mostly in

the 3'-most exon, can alter transcript stability,<sup>9,14</sup> localization,<sup>15</sup> translation efficiency,<sup>16</sup> and protein complex formation.<sup>12</sup> In addition, PAS usage upstream of the 3'-most exon, chiefly in introns, diversifies the proteome by producing C-terminally truncated proteins with distinct functions<sup>10,11</sup> or leads to unstable transcripts, inhibiting gene expression. APA plays a critical role in normal cellular differentiation and cancer transformation. Global PAS profiling reveals that transcript expression signatures shift from proximal to distal PAS usage during normal cellular differentiation.<sup>17-19</sup> The opposite shift occurs during cellular transformation, linking transcript shortening to proliferative cellular states.<sup>9,20-23</sup>

Thus far, the mechanistic link between APA alteration and oncogenic transformation is incomplete. One common explanation is that 3'UTR shortening contributes to oncogene upregulation when affected transcripts evade normal miRNA-mediated degradation.<sup>9,14</sup> In addition, global coding sequence (CDS) shortening by enhanced usage of intronic PASs reportedly inactivates tumor

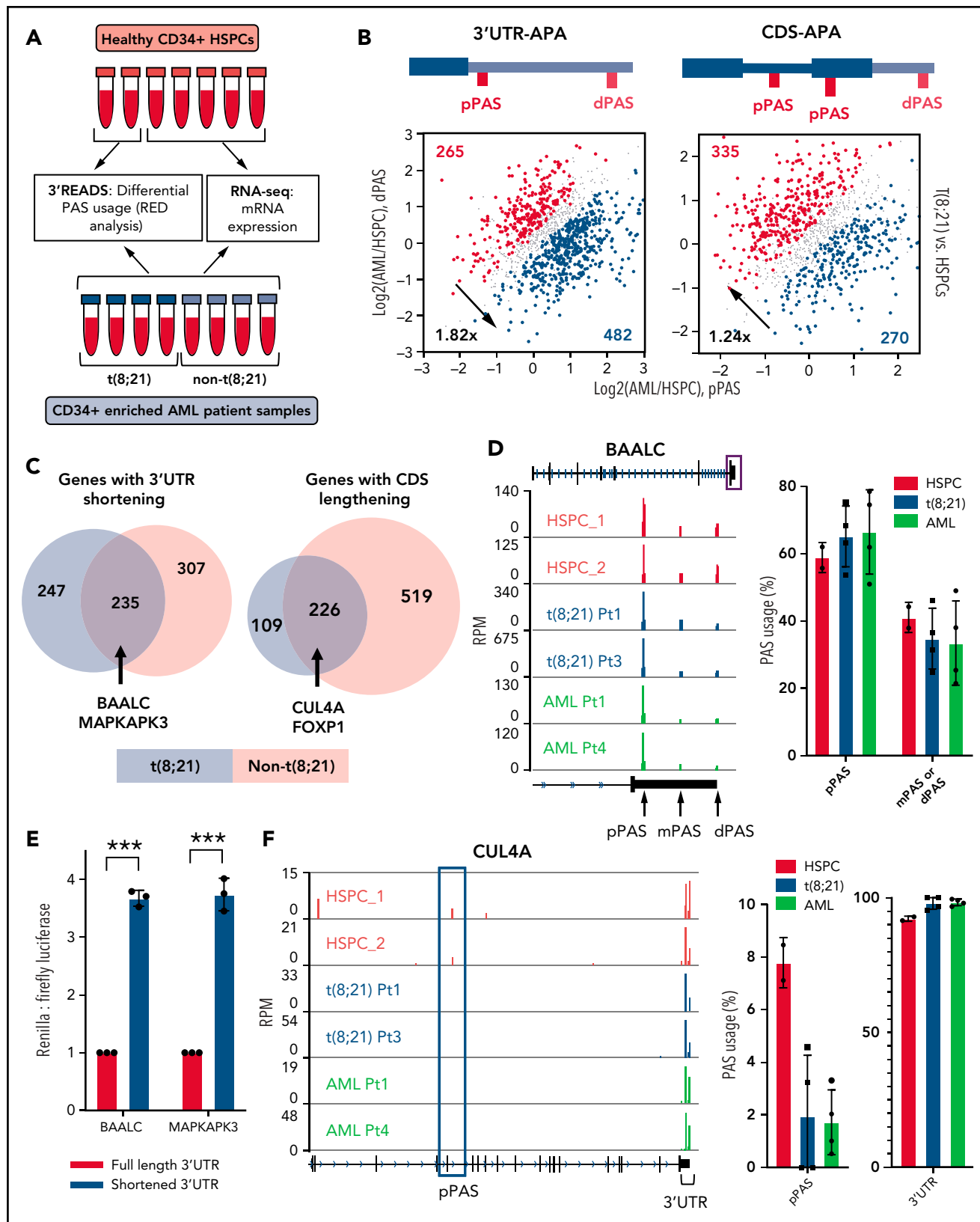


**Figure 1. Alternative polyadenylation is apparent in AML patient samples, affecting genes that promote leukemia development.** (A) Schematic of AML patient samples and healthy HSPCs used for 3'READS and/or RNA-sequencing. (B) Scatter plot showing the change in expression of the proximal poly(A) site (pPAS) isoform (x-axis) and distal poly(A) site (dPAS) isoform (y-axis), per gene, in t(8;21) AML patient blasts compared with healthy HSPCs. Significant APA events (Fisher's exact test,  $P < .05$ ) are classified and divided according to type: 3'UTR-APA (left) and CDS-APA (right). Blue dots indicate significantly more pPAS usage; red dots indicate significantly more dPAS usage. (C) Venn diagrams showing the overlap of genes with 3'UTR shortening and CDS lengthening in t(8;21) AML blasts and non-t(8;21) AML blasts compared with healthy HSPCs. (D) Genome browser tracks depicting normalized sequencing reads

suppressor genes in cancer cells.<sup>11</sup> Although these have been shown for some genes, oncogenes do not always have shorter 3'UTRs, and tumor suppressors are not the only genes that have shorter CDS due to APA. Thus, the collective contribution of global APA dysregulation on cellular transformation is still elusive.

Acute myeloid leukemia (AML) is a cancer characterized by a hallmark block in differentiation.<sup>24</sup> Consequently, there is great clinical interest in developing therapies that promote differentiation of leukemia cells. Among reported differentiating agents, success has been limited to all-trans retinoic acid<sup>25</sup> and arsenic trioxide<sup>26</sup> in patients with acute promyelocytic leukemia (APL), and more recently isocitrate dehydrogenase (IDH) inhibitors in patients with IDH-mutant AML.<sup>27-29</sup> Despite the promising efficacy of these therapies, the percentage of patients that can benefit from them is limited. It is therefore clinically important to identify additional targetable pathways mediating the differentiation block of AML.

Here, we analyzed PAS usage in several AML patient subtypes compared with healthy hematopoietic cells and report global dysregulation of APA in myeloid leukemia. Among the core cleavage and polyadenylation factors, we found that *FIP1L1* messenger RNA (mRNA) expression was correlated with 3'UTR shortening in the patient cohort we examined by using 3' region extraction and deep sequencing (3'READS). Disruption of global APA dysregulation by *FIP1L1* knockdown led to leukemia cell differentiation, supporting an underappreciated role of APA in blocking the normal maturation of cancer cells. We also identified 3'UTR-APA regulation of *AML1-ETO* expression, a key AML oncofusion gene that contributes to this observed differentiation block. Finally, by disrupting global APA patterns, we detected downregulation of *MYC* and mechanistic target of rapamycin complex 1 (mTORC1) signaling across AML cells of diverse mutational contexts, linking dysregulated APA to leukemia cell phenotypes. Our findings underline the importance of posttranscriptional mechanisms in leukemia development and propose APA as a putative therapeutic target for inducing differentiation in patients with AML.

## Methods

A complete description of all methods is presented in the supplemental Methods (available on the *Blood* Web site).

### Primary patient samples and healthy hematopoietic stem and progenitor cells

AML samples were obtained from patients at UC San Diego Health with written consent and in accordance with a university-approved Institutional Review Board protocol. After collection of peripheral blood or bone marrow, cells were separated by using Ficoll-Paque (17-1440-02; VWR) and frozen until further use.

Patient cells were thawed quickly at 37°C, diluted in 1× phosphate-buffered saline supplemented with 1 mg/mL DNase (1184932001; Sigma) and washed with 1× phosphate-buffered saline supplemented with 2% fetal bovine serum. Live, mononuclear cells were separated by using Ficoll-Paque and washed again. Magnetic bead CD34 enrichment was performed by using the MACS Miltenyi Kit (130-046-702). An aliquot of CD34-enriched leukemic blasts was analyzed by using flow cytometry to confirm that cells were >95% CD34<sup>+</sup>. RNA was extracted from patient blasts using TRIzol reagent (15596026; Thermo Fisher Scientific).

Cryopreserved, previously enriched CD34<sup>+</sup> hematopoietic stem and progenitor cells (HSPCs) from healthy donors were obtained from Fred Hutchinson Cooperative Center for Excellence in Hematology. All HSPC samples were >95% CD34<sup>+</sup>. Cells were thawed quickly and serially diluted with 1× phosphate-buffered saline supplemented with 2% fetal bovine serum. Cells were resuspended in TRIzol for RNA extraction.

## Results

### APA is globally dysregulated in patients with AML

To assess the prevalence of APA dysregulation in AML, we first performed 3'READS<sup>30,31</sup> and standard RNA-sequencing on enriched AML patient blasts (CD34<sup>+</sup>) and healthy HSPCs (Figure 1A; supplemental Figure 1A-B). Because blasts from patients with AML are heterogeneous, we selected 4 patient samples that commonly carried the t(8;21) translocation generating the *AML1-ETO* fusion oncoprotein and 4 non-t(8;21) samples with variable mutations (supplemental Table 1). Compared with healthy HSPCs, both groups of patients exhibited dysregulated APA of numerous genes with an overall trend of 3'UTR shortening, which has been reported in various cancer types<sup>14,22</sup> (Figure 1B; supplemental Figure 1C). Patient blasts also exhibited CDS lengthening, which was similarly seen in multiple myeloma samples.<sup>10</sup> However, both trends are opposite of those reported in chronic lymphocytic leukemia samples,<sup>11,12</sup> highlighting the importance of disease-specific PAS profiling. To further study APA trends in a broader cohort of patients with AML, we analyzed the publicly available BeatAML data set. Across patient subsets, defined by the presence or absence of common AML fusion proteins, 3'UTR shortening was observed in patients compared with healthy bone marrow (supplemental Figure 2A). CDS lengthening was also seen in most patient groups, supporting the prevalence of this trend across AML subtypes (supplemental Figure 2B).

### Dysregulated APA affects oncogenic pathways and genes in patients with AML

In our 3'READS data set, many genes were similarly shortened or lengthened in t(8;21) and non-t(8;21) patients (Figure 1C). To

**Figure 1 (continued)** (reads per million [RPM]) in the *BAALC* gene obtained from 3'READS of HSPCs and AML patient blasts. The full *BAALC* genomic structure is shown (top) with the purple, boxed region expanded (below). The percent usage of each indicated PAS was calculated by using 3'READS and is shown in the bar graph to the right. n = 2, HSPCs; n = 4, t(8;21) and non-t(8;21) AML patient samples. (E) Relative ratio of *Renilla* to firefly luciferase activity in Kasumi-1 cells nucleofected with the indicated dual luciferase reporter. Red bars represent activity when the full 3'UTR of the indicated gene was subcloned downstream of *Renilla* luciferase; blue bars represent activity when the shortened 3'UTR was present. Data are mean ± standard deviation of 3 independent experiments. \*\*\*P < .001, Student t test. (F) Genome browser tracks depicting normalized sequencing reads (RPM) in the *CUL4A* gene obtained from 3'READS of HSPCs and AML patient blasts. The proximal, intronic PAS is boxed. The percent usage of each indicated PAS was calculated by using 3'READS and is shown in the bar graph to the right. n = 2, HSPCs; n = 4, t(8;21) and non-t(8;21) AML patient samples.

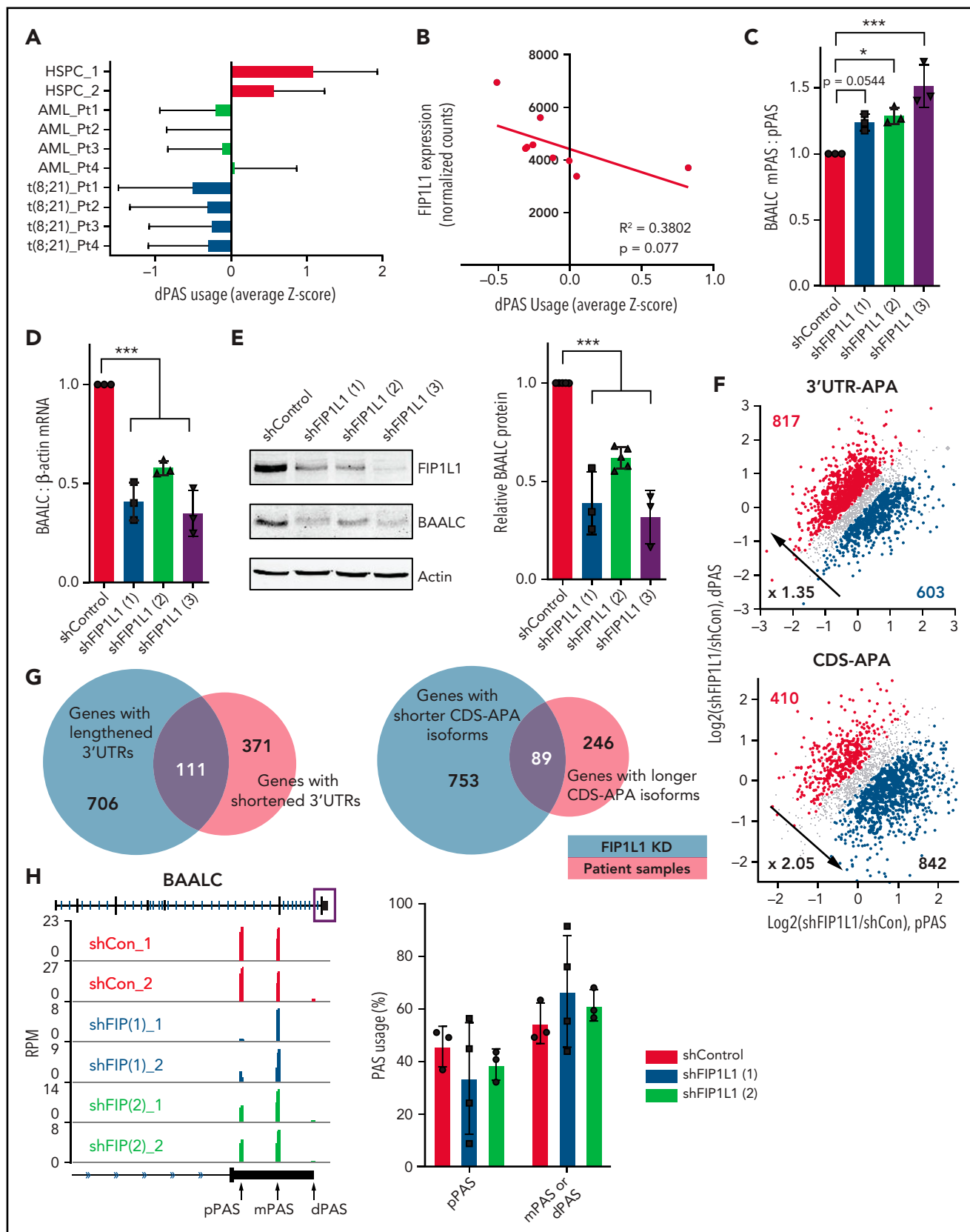


**Figure 2. Targeting FIP1L1 reverses APA trends in t(8;21) AML.** (A) Extent of 3'UTR shortening, in all patient samples and primary HSPC controls, of the 235 genes with shortened 3'UTRs in both t(8;21) and non-t(8;21) patients. For each gene, the average and standard deviation (SD) of dPAS usage were determined. Z scores were then calculated and assigned to each sample in the cohort for the given gene. Each bar of the graph represents the average z score of all 235 genes in the indicated patient or healthy control, a measure of the overall degree of shortening. Data are mean  $\pm$  SD. (B) Negative correlation between FIP1L1 expression, calculated by RNA-sequencing, and the extent of 3'UTR shortening per patient. Among all APA regulators, FIP1L1 expression is most correlated to 3'UTR shortening. Correlation was

evaluate whether the observed changes in APA might contribute to pathogenesis, pathway enrichment was performed on the common genes that exhibited 3'UTR shortening or CDS lengthening. Significantly enriched pathways included those related to cell cycle, differentiation, and oncogenic signaling pathways, supporting a likely role of APA in leukemia (supplemental Table 2). We next sought to identify specific genes with altered PAS usage that might contribute to disease. 3'UTR-APA regulates gene expression by altering the presence of 3'UTR regions that bind miRNAs or RNA-binding proteins (RBPs), which modulate transcript stability and/or translation efficiency.<sup>17,32</sup> In cancer, global 3'UTR shortening by APA reportedly induces oncogene upregulation by transcript evasion of miRNAs or suppressive RBPs.<sup>9,14,16,33</sup> Among genes that exhibited significant 3'UTR shortening in our 3'READS data set, we identified *BAALC*, a negative prognostic marker in AML<sup>34,35</sup> that blocks AML cell differentiation,<sup>36,37</sup> and *MAPKAPK3*, a MAPK signaling node that contributes to the characteristic differentiation block of t(8;21) AML<sup>38</sup> (Figure 1D; supplemental Figure 3A-C). Because 3'UTR length is not always predictive of protein output,<sup>39,40</sup> we tested whether 3'UTR length can contribute to the expression of these leukemia-promoting genes. We subcloned the short and long 3'UTR variants downstream of Renilla luciferase in a dual luciferase reporter and compared the effect on protein output. For both genes, the shorter 3'UTR produced significantly more Renilla protein than the longer 3'UTR, confirming a direct role of APA on gene expression (Figure 1E).

As with 3'UTR-APA, intronic APA can also affect gene expression when premature cleavage and polyadenylation results in a truncated protein product that lacks crucial functional domains.<sup>11,41</sup> In cancer, global CDS shortening by intronic polyadenylation inactivates tumor suppressor genes.<sup>11</sup> We observed the opposite overall trend of CDS lengthening in patients with AML and reasoned that activation of oncogenes is also a possibility. Among genes with significant CDS lengthening in our 3'READS data set, we identified *CUL4A*, an oncogenic E3 ubiquitin ligase that promotes proliferation and blocks differentiation in hematopoietic models.<sup>42,43</sup> We also identified *FOXP1*, a transcription factor that is a negative prognostic marker in patients with AML,<sup>44</sup> suppresses cell cycle inhibitors in myeloid leukemia cells,<sup>45</sup> and plays an oncogenic role in diffuse large B-cell lymphoma<sup>46</sup> (Figure 1F; supplemental Figure 3D-F). Usage of the proximal intronic PAS in each case would result in a severely

truncated protein that is expected to be dysfunctional<sup>10</sup> (supplemental Figure 3G). Altogether, we saw pronounced differences in PAS usage between patient blasts and healthy control subjects and identified specific genes that could reasonably contribute to pathogenesis.

### Targeting *FIP1L1* reverses APA trends in t(8;21) AML

Although altered posttranscriptional regulation of individual gene targets contributes to oncogenic transformation, the sum of small changes can also collectively promote pathogenesis. We therefore wanted to test whether targeting global polyadenylation patterns might have antileukemic effects. We first selected a common APA regulator to target by using our patient 3'READS and RNA-sequencing data sets. Because 3'UTR shortening is a common feature observed in many cancer types<sup>22,47</sup> and is also seen in our data set, we focused on the severity of shortening per patient of the overlapping 235 genes (Figure 2A; supplemental Figure 4). We observed noticeable differences in the extent of 3'UTR shortening across this set of genes, and calculated the correlation between the degree of shortening and the expression level of all APA machinery members in each patient. High *FIP1L1* expression was identified as being most predictive of 3'UTR shortening (Figure 2B; supplemental Table 3). We also examined the publicly available AML data set but did not observe a broad correlation between *FIP1L1* expression and 3'UTR length, suggesting that additional APA regulators likely contribute to APA dysregulation in different patients. However, because *FIP1L1* knockdown induces 3'UTR lengthening in murine systems,<sup>48,49</sup> we selected *FIP1L1* as a model APA regulator to test the hypothesis that targeting global APA dysregulation may be detrimental to leukemia cells.

We selected the t(8;21)-positive Kasumi-1 cell line as a suitable model because we observed more pronounced shortening in the t(8;21) vs non-t(8;21) patients in our cohort (Figure 2A). *FIP1L1* knockdown promoted 3'UTR lengthening of *BAALC* (Figure 2C) that corresponded to significant downregulation of *BAALC* mRNA (Figure 2D) and protein (Figure 2E), a change with potential clinical significance. We next tested whether *FIP1L1* knockdown could globally alter the APA dysregulation we observed in patients. We performed short hairpin RNA (shRNA)-mediated knockdown in Kasumi-1 cells and observed global 3'UTR lengthening but CDS shortening, a reversal of the

**Figure 2 (continued)** determined by linear regression. (C) Reverse transcription quantitative polymerase chain reaction (RT-qPCR) analysis of *BAALC* 3'UTR length in Kasumi-1 cells transduced with shRNAs targeting *FIP1L1* [shRNA (1), (2), or (3)] or a control shRNA. Usage of either the middle or distal PAS was measured relative to total *BAALC* mRNA using primer pairs upstream of the middle poly(A) site (mPAS) and most proximal poly(A) site (pPAS), respectively. Relative 3'UTR length in *FIP1L1* knockdown Kasumi-1 cells was normalized to 3'UTR length in cells transduced with the control shRNA. Data are mean  $\pm$  SD of 3 independent experiments. \* $P < .05$ , \*\*\* $P < .001$ , 1-way analysis of variance (ANOVA) with a post hoc Tukey test. (D) RT-qPCR analysis of total *BAALC* mRNA normalized to  $\beta$ -Actin mRNA in Kasumi-1 cells upon shRNA knockdown of *FIP1L1*. mRNA levels in knockdown cells were normalized to cells transduced with the control shRNA. Data are mean  $\pm$  SD of 3 independent experiments. \*\*\* $P < .001$ , one-way ANOVA with a post hoc Tukey test. (E) Western blot showing *FIP1L1*, *BAALC*, and actin (loading control) protein in Kasumi-1 cells after transduction with control shRNAs or shRNAs targeting *FIP1L1*. *BAALC* protein was quantified by normalizing *BAALC* signal intensity to actin signal intensity using Li-Cor Image Studio software. Normalized protein quantifications are shown in the bar graph to the right.  $n = 5$  for shControl and sh*FIP1L1* (2);  $n = 3$  for sh*FIP1L1* (1) and sh*FIP1L1* (3). Data are mean  $\pm$  SD. \*\*\* $P < .001$ , 1-way ANOVA with a post hoc Tukey test. (F) Scatter plot showing the change in expression of pPAS and dPAS isoforms, per gene, in Kasumi-1 cells after *FIP1L1* knockdown. Significant differences in PAS usage were calculated by using the Fisher's exact test, comparing PAS usage in Kasumi-1 cells transduced with both shRNAs targeting *FIP1L1* vs the control shRNA. APA events are classified and divided according to type: 3'UTR-APA (top) and CDS-APA (bottom). Each dot corresponds to a single gene. Blue dots indicate significantly more pPAS usage; red dots indicate significantly more dPAS usage. (G) Venn diagrams showing: (left) the overlap of genes with 3'UTR shortening in t(8;21) AML blasts that were significantly lengthened upon *FIP1L1* knockdown in Kasumi-1 cells and (right) the overlap of genes with CDS lengthening in t(8;21) AML blasts that were significantly shortened upon *FIP1L1* knockdown in Kasumi-1 cells. (H) Genome browser tracks depicting normalized sequencing reads (reads per million [RPM]) in the *BAALC* gene obtained from 3'READS of Kasumi-1 cells transduced with a control shRNA or shRNAs targeting *FIP1L1*. The full *BAALC* genomic structure is shown (top) with the purple, boxed region expanded (below). The percent usage of each indicated PAS was calculated by using 3'READS and is shown in the bar graph to the right.  $n = 3$ , shControl and sh*FIP1L1* (2);  $n = 4$  sh*FIP1L1* (1).



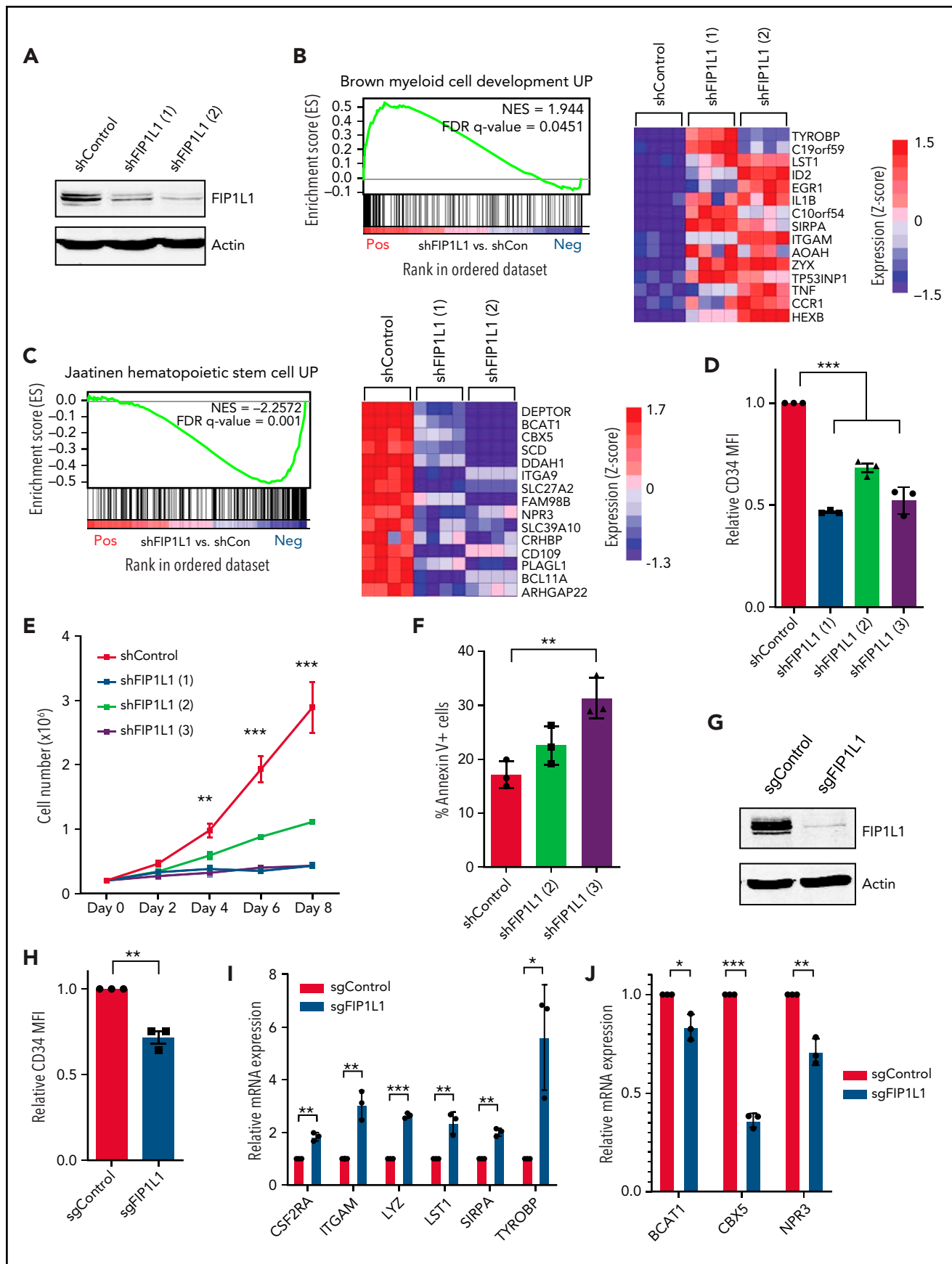


Figure 3.

trends observed in AML patient blasts (Figure 2F). Importantly, 23% of the genes that had shorter 3'UTRs as detected by using 3'READS in our patient samples were lengthened upon FIP1L1 knockdown and 27% of genes with longer CDS-APA isoforms were shortened upon FIP1L1 knockdown (Figure 2G). BAALC was among the former group, confirming our previous finding (Figure 2H). Altogether, these results show the feasibility of altering global APA profiles by targeting a strategically selected APA regulator.

### FIP1L1 knockdown promotes t(8;21) leukemic cell differentiation

We next performed RNA-sequencing of FIP1L1 knockdown Kasumi-1 cells to determine whether the perturbation of global APA patterns had an antileukemic effect (Figure 3A; supplemental Figure 5A). Targeting this APA regulator profoundly changed global gene expression, highlighting the interplay between post-transcriptional gene regulation and transcriptome composition (supplemental Figure 5B). Gene set enrichment analysis (GSEA) revealed that genes which were upregulated upon FIP1L1 knockdown significantly matched those that are upregulated upon myeloid cell development. This included genes such as *ITGAM* (CD11b)<sup>50</sup> and *LST1*,<sup>51</sup> classical markers of mature myeloid cells (Figure 3B). Similarly, genes that were downregulated upon FIP1L1 knockdown negatively correlated with those that are typically upregulated in HSCs. Among these genes are reported leukemic oncogenes *BCAT1*<sup>52,53</sup> and *CBX5*<sup>54</sup> (Figure 3C). Flow cytometric analysis of Kasumi-1 cells revealed that FIP1L1 knockdown reduced CD34 cell surface expression, indicative of a more differentiated cellular state (Figure 3D; supplemental Figure 5C). This change correlated with a decrease in cell proliferation (Figure 3E) and an increase in apoptosis (Figure 3F). We confirmed the differentiation phenotype by using a single guide RNA (sgRNA) that targets exon 1 of FIP1L1 (Figure 3G; supplemental Figure 5D). With this orthogonal method of knockdown, we again observed decreased CD34 cell surface expression (Figure 3H; supplemental Figure 5E), an increase in expression of myeloid differentiation genes (Figure 3I), and a decrease in stem cell signature genes (Figure 3J). Overall, our results indicate that targeting APA promotes t(8;21) leukemia cell differentiation.

### 3'UTR-APA regulates AML1-ETO expression

We next wondered whether we could identify an individual APA event altered by targeting FIP1L1 that might contribute to the

differentiation phenotype observed. Indeed, among the genes with significantly altered APA was the t(8;21) generated fusion oncoprotein AML1-ETO. FIP1L1 knockdown induced AML1-ETO 3'UTR lengthening (Figure 4A-B; supplemental Figure 5F). We observed a decrease in usage of the proximal PAS at 1 kb, a concurrent increase in usage of the 3.7 kb site, and the emergence of usage at the most distal 5.2 kb site. To confirm that FIP1L1 directly regulates ETO APA, we overexpressed FIP1L1 in 293T cells using a doxycycline-inducible construct and observed shortening of the ETO 3'UTR after 24 hours of induction (Figure 4C-D).

Supporting the functional relevance of this APA event, 3'UTR lengthening in FIP1L1 knockdown Kasumi-1 cells corresponded to downregulation of AML1-ETO protein (Figure 4E) and the reversal of downstream target genes (Figure 4F). Because AML1-ETO plays a well-defined role in blocking differentiation of t(8;21) AML patients,<sup>55-59</sup> it is one of several genes contributing to the differentiation phenotype seen upon FIP1L1 knockdown in t(8;21) cells. To confirm that 3'UTR length of the AML1-ETO transcript contributes to protein production, we again performed luciferase assays comparing Renilla luciferase production when followed by the 1 kb, 3.7 kb, or 5.2 kb ETO 3'UTR. Indeed, the shortest 1 kb 3'UTR produced 7 to 8 times more Renilla luciferase activity than either the 3.7 or 5.2 kb 3'UTR (Figure 4G). This observation is supported by various reports of miRNAs that bind to the 3'UTR region downstream of the 1 kb PAS and downregulate AML1-ETO.<sup>60-62</sup> Finally, t(8;21) AML patient samples have significantly higher *FIP1L1* expression than non-t(8;21) patients in 2 large data sets,<sup>63,64</sup> further supporting a role for this specific APA regulator in maintaining expression of AML1-ETO in patients (supplemental Figure 6). Importantly, our data show that a fusion oncoprotein is susceptible to APA-mediated gene expression regulation.

### FIP1L1 expression correlates with cell maturity across AML

Although t(8;21) AML patients tended to have higher *FIP1L1* expression, some non-t(8;21) patients also had elevated *FIP1L1* expression. Therefore, we hypothesized that targeting APA by FIP1L1 knockdown might apply more broadly to patients with AML. To address this, we used the publicly available RNA-sequencing data of The Cancer Genome Atlas patient cohort<sup>63</sup> and performed differential gene expression analysis of the highest and lowest *FIP1L1*-expressing patients (Figure 5A). Gene

**Figure 3. FIP1L1 knockdown promotes t(8;21) leukemic cell differentiation.** (A) Western blot showing FIP1L1 and actin (loading control) protein in Kasumi-1 cells after transduction with control shRNAs or shRNAs targeting *FIP1L1*. (B) GSEA plot comparing differentially expressed genes upon FIP1L1 knockdown in Kasumi-1 cells with the Brown Myeloid Cell Development UP gene set. The heatmap displays 15 genes in the leading edge of the gene set that are most upregulated upon FIP1L1 knockdown. (C) GSEA plot comparing differentially expressed genes upon FIP1L1 knockdown in Kasumi-1 cells with the Jaatinen Hematopoietic Stem Cell UP gene set. The heatmap displays 15 genes in the leading edge of the gene set that are most downregulated upon FIP1L1 knockdown. (D) CD34 cell surface expression measured by flow cytometry of Kasumi-1 cells 6 days after transduction with shRNAs targeting *FIP1L1* or a control shRNA. Data are mean  $\pm$  standard deviation (SD) of 3 independent experiments. \*\*\* $P < .001$ , 1-way analysis of variance (ANOVA) with post hoc Tukey test. (E) Proliferation of Kasumi-1 cells after transduction with shRNAs targeting *FIP1L1* or a control shRNA. Cells were seeded (day 0) after 2 days of puromycin selection. The graph displays the mean and SD of 3 technical replicates in 1 representative experiment of 2 independent experiments. \*\* $P < .01$ , \*\*\* $P < .001$ , multiple Student *t* tests using the Holm-Sidak method. (F) Percentage of Annexin V-positive apoptotic Kasumi-1 cells 5 days after transduction with shRNAs targeting *FIP1L1* or control shRNAs. Data are mean  $\pm$  SD of 3 independent experiments. \*\* $P < .01$ , 1-way ANOVA with post hoc Tukey test. (G) Western blot showing FIP1L1 and actin (loading control) protein in Kasumi-1 cells after transduction with control sgRNAs targeting green fluorescent protein or sgRNAs targeting *FIP1L1*. (H) CD34 cell surface expression measured by flow cytometry of Kasumi-1 cells 10 days after transduction with sgRNAs targeting *FIP1L1* or control sgRNAs. Data are mean  $\pm$  SD of 3 independent experiments. \*\* $P < .01$ , Student *t* test. (I) Reverse transcription quantitative polymerase chain reaction (RT-qPCR) analysis of various myeloid differentiation genes in Kasumi-1 cells transduced with sgRNAs targeting *FIP1L1* or control sgRNAs. Data are mean  $\pm$  SD of 3 independent experiments. \* $P < .05$ , \*\* $P < .01$ , \*\*\* $P < .001$ , multiple Student *t* tests using the Holm-Sidak method. (J) RT-qPCR analysis of various HSC signature genes in Kasumi-1 cells transduced with sgRNAs targeting *FIP1L1* or control sgRNAs. Data are mean  $\pm$  SD of 3 independent experiments. \* $P < .05$ , \*\* $P < .01$ , \*\*\* $P < .001$ , multiple Student *t* tests using the Holm-Sidak method. FDR, false discovery rate; MFI, mean fluorescent intensity; NES, normalized enrichment score.

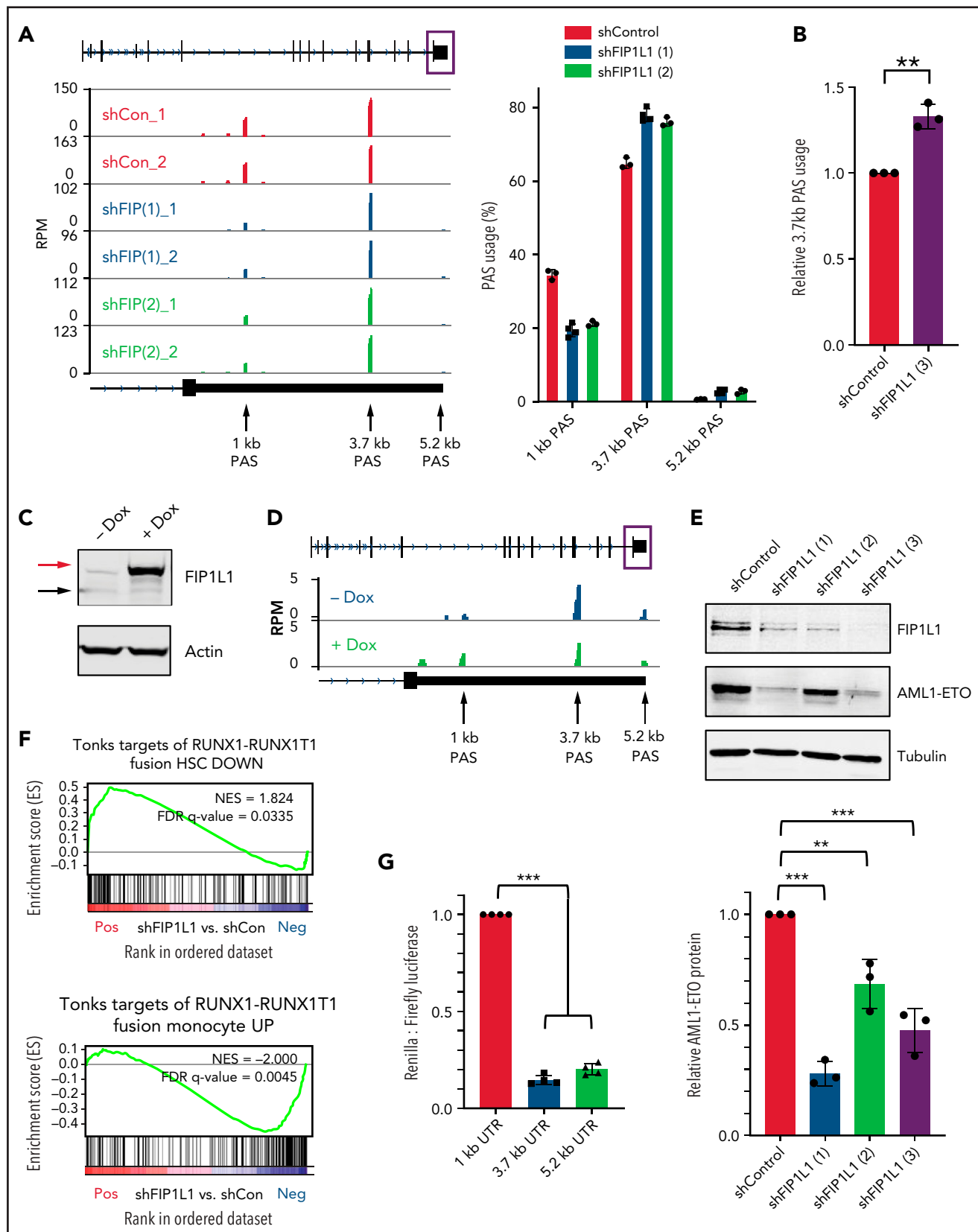


**Figure 4. 3'UTR-APA regulates AML1-ETO expression.** (A) Genome browser tracks depicting normalized sequencing reads (reads per million [RPM]) in the *RUNX1T1* (aka *ETO*) gene obtained from 3'READS of Kasumi-1 cells transduced with a control shRNA or shRNAs targeting *FIP1L1* [shRNA (1) or (2)]. The full *RUNX1T1* genomic structure is shown (top) with the purple, boxed region expanded (below). The percent usage of each indicated PAS was calculated by using 3'READS and is shown in the bar graph to the right.  $n = 3$ , shControl and shFIP1L1 (2);  $n = 4$  shFIP1L1 (1). (B) Reverse transcription quantitative polymerase chain reaction (RT-qPCR) analysis of *AML1-ETO* 3'UTR length in Kasumi-1 cells transduced with a third, unique shRNA (3) targeting *FIP1L1* or a control shRNA. Usage of the PAS at 3.7 kb was measured



ontology analysis of pathways enriched in *FIP1L1* low-expressing patients revealed a striking overlap with those that were enriched upon *FIP1L1* knockdown in t(8;21)<sup>+</sup> Kasumi-1 cells. Importantly, overlapping enriched pathways support a gene expression signature of leukocyte differentiation (Figure 5B). GSEA analysis further revealed that high-expressing *FIP1L1* patients had gene expression profiles positively correlated with both immature HSCs and leukemic stem cells (Figure 5C). When stratified according to FAB subtype, *FIP1L1* expression was significantly higher in M0-M2 vs M3-M6 leukemia patients (supplemental Figure 7A). Collectively, these data support a role of *FIP1L1* in regulating stemness gene signatures in patients and prompted us to evaluate the impact of *FIP1L1* knockdown in a non-t(8;21) AML context. We turned to the HL-60 and NB4 cell lines, classically used to model myeloid cell differentiation. *FIP1L1* knockdown (Figure 5D) resulted in the robust emergence of CD11b<sup>+</sup> cells (Figure 5E; supplemental Figure 8A) and the corresponding nuclear morphology of granulocyte differentiation (Figure 5F; supplemental Figure 8B). This differentiation phenotype was confirmed in both cell lines by sgRNA knockdown of *FIP1L1* (supplemental Figure 8C-E). This phenotype was induced without the addition of traditional differentiating agents, supporting a profound role of targeting APA and overcoming the hallmark differentiation block of AML. Finally, we observed decreased proliferation (Figure 5G) and increased apoptosis (Figure 5H) of these 2 cell lines upon *FIP1L1* knockdown, much like we observed in Kasumi-1 cells.

### Targeting APA converges on MYC expression and mTORC1 signaling

Because non-t(8;21) cells also differentiated upon *FIP1L1* knockdown, we reasoned that common leukemia-promoting pathways must be altered that do not exclusively rely on AML1-ETO protein expression. To identify such pathways, we returned to our RNA-sequencing data from *FIP1L1* knockdown in Kasumi-1 cells. Pathway analysis of significantly downregulated genes revealed a striking reduction in biosynthetic processes (Figure 6A). GSEA clarified this general observation as an overall reduction in mTORC1 signaling, a pathway that is constitutively active in leukemia, contributing to initiation and progression.<sup>65-67</sup> Specifically, genes downregulated upon *FIP1L1* knockdown matched those that are downregulated upon treatment with rapamycin, an mTORC1 inhibitor (Figure 6B). To test whether *FIP1L1* knockdown commonly attenuates mTORC1 signaling across AML, shRNA-mediated knockdown was performed in 5 mutationally diverse AML cell lines, and a reduction in phosphorylated p70-S6 Kinase 1 (S6K1), the rapamycin-sensitive direct downstream target of mTOR kinase,<sup>68,69</sup> was observed (Figure 6C).

Attenuation of mTORC1 signaling regulates myeloid differentiation through translational control of the MYC transcription factor.<sup>70</sup> Indeed, we also saw potent downregulation of MYC target genes in our *FIP1L1* knockdown RNA-sequencing data set (Figure 6A,D; supplemental Figure 9A). We confirmed that MYC protein is reduced in all 5 AML cell lines (Figure 6E). Taken together, targeting APA induced differentiation and reduced proliferation (supplemental Figure 8F) across AML subtypes by downregulating global oncogenic signaling pathways.

## Discussion

We have added to a growing field of knowledge regarding APA dysregulation in cancer. By examining PAS usage in patients with AML compared with healthy control subjects, we showed that, due to APA, patients exhibited global 3'UTR shortening but CDS lengthening. To study the impact of this global APA dysregulation in leukemia, we targeted *FIP1L1*, the APA regulator whose mRNA levels correlated with 3'UTR shortening in our 3'READS AML patient cohort. We discovered that APA dysregulation contributes to the differentiation block of leukemia cells, described the impact of APA on the expression of crucial oncogenes, and introduced APA as a putative therapeutic target in AML.

Our results highlight the potential of targeting an APA regulator to overcome the hallmark differentiation block of leukemia. Despite the importance of APA in modulating healthy cellular differentiation,<sup>17-19</sup> the role of dysregulated APA in cancer has been predominantly attributed to its impact on cellular proliferation.<sup>9,20,22,23</sup> Various studies report 3'UTR shortening and upregulation of cell-cycle and proliferation-related transcripts in cancer such as *CCND1*<sup>14,21,71</sup> and *CDC6*.<sup>33</sup> Although not excluding the effects on differentiation, these studies imply that reduced differentiation is a byproduct of enhanced proliferation. However, non-transformed cells with similar proliferative capacity as transformed cells do not exhibit the same 3'UTR shortening, supporting an oncogenic role for APA that is proliferation independent.<sup>14</sup> The current study addresses this knowledge gap and emphasizes a role of APA in mediating differentiation of cancer cells. Targeting global APA dysregulation by *FIP1L1* knockdown induced differentiation of mutationally diverse AML cell lines. In patients, *FIP1L1* expression was correlated to leukemia cell maturation, supporting the clinical relevance of this finding. Mechanistically, we identified 3'UTR-APA of the t(8;21) fusion protein AML1-ETO, reporting for the first time that APA can affect expression of a prominent oncofusion. Importantly, AML1-ETO is implicated in the differentiation block, but not the enhanced proliferation, of myeloid leukemia cells.<sup>55</sup> We also experimentally

**Figure 4 (continued)** relative to total AML1-ETO mRNA using primer pairs upstream of the 3.7 kb PAS and 1 kb PAS, respectively. Data are mean  $\pm$  standard deviation (SD) of 3 independent experiments. \*\**P* < .01, Student *t* test. (C) Western blot showing *FIP1L1* and actin (loading control) protein in 293T cells transfected with a FLAG-tagged, doxycycline (Dox)-inducible *FIP1L1* overexpression construct, with and without 1  $\mu$ g/mL Dox in the culture medium for 24 hours. The black arrow indicates endogenous *FIP1L1*. The red arrow indicates FLAG-tagged *FIP1L1*. (D) Genome browser tracks depicting normalized sequencing reads (RPM) in the *RUNX1T1* (aka *ETO*) gene obtained from 3'READS of 293T cells transfected with a Dox-inducible *FIP1L1* overexpression construct, with and without 1  $\mu$ g/mL Dox in the culture medium for 24 hours. The full *RUNX1T1* genomic structure is shown (top) with the purple, boxed region expanded (below). (E) Western blot showing *FIP1L1*, AML1-ETO, and tubulin (loading control) protein in Kasumi-1 cells after transduction with control shRNAs or shRNAs targeting *FIP1L1*. AML1-ETO protein was quantified by normalizing AML1-ETO signal intensity to tubulin signal intensity using LI-COR Image Studio software. Normalized protein quantifications from 3 independent experiments are shown in the bar graph below. Data are mean  $\pm$  SD. \*\**P* < .01, \*\*\**P* < .001, one-way analysis of variance (ANOVA) with a post hoc Tukey test. (F) Plots from GSEA of the RNA-sequencing experiment shown in Figure 3A (supplemental Figure 5A-B). The top plot displays genes that are downregulated by AML1-ETO; the bottom plot displays those that are upregulated by AML1-ETO. (G) Relative ratio of Renilla to firefly luciferase in Kasumi-1 cells nucleofected with the indicated dual luciferase reporter construct containing variable *RUNX1T1* (aka *ETO*) 3'UTRs. Data are mean  $\pm$  SD of 4 independent experiments. \*\*\**P* < .001, 1-way ANOVA with a post hoc Tukey test. FDR, false discovery rate; NES, normalized enrichment score.

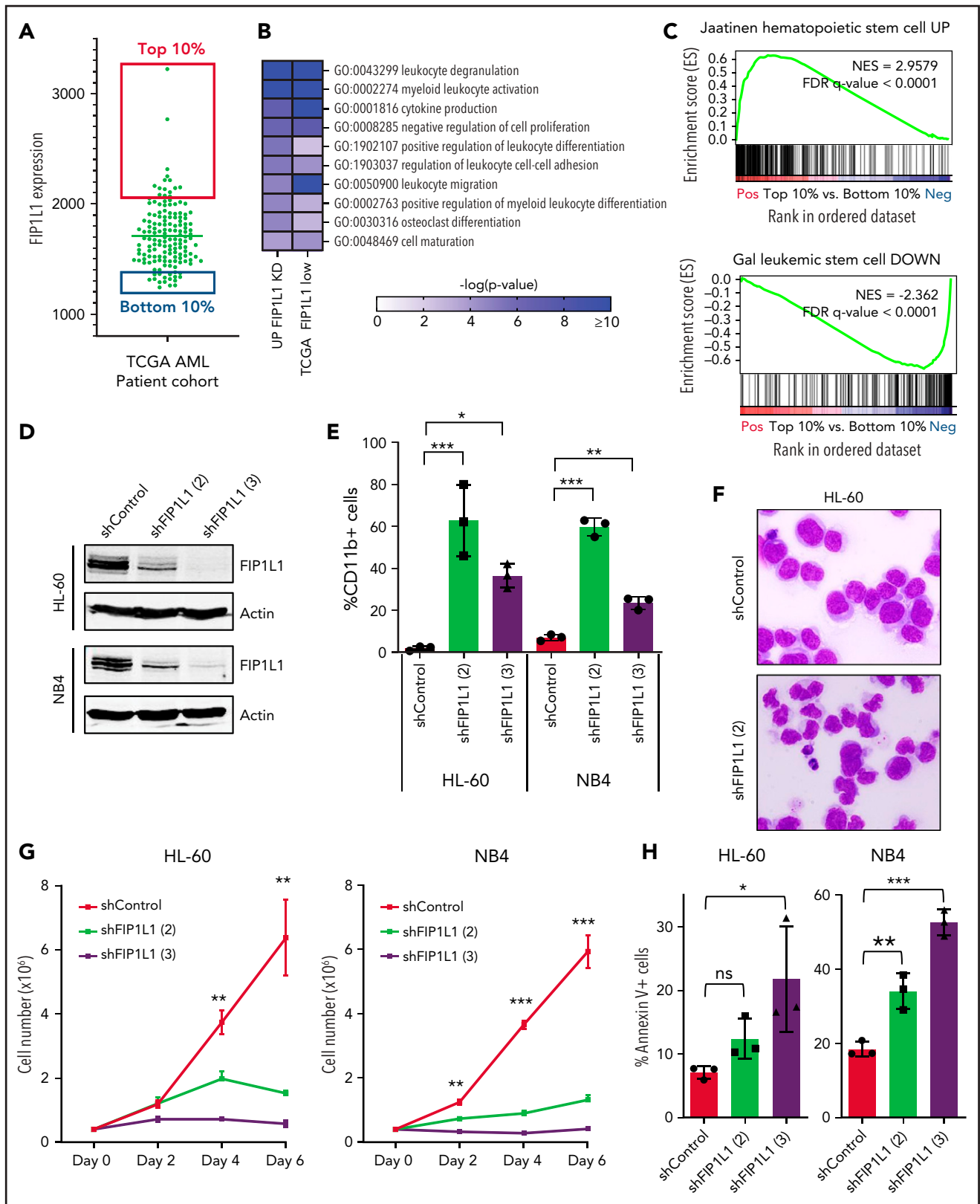


**Figure 5. *FIP1L1* expression correlates to stemness gene signatures and differentiation across AML.** (A) Box and whisker plot depicting the *FIP1L1* expression of all patients in the AML patient cohort of The Cancer Genome Atlas (TCGA). Differential gene expression analysis was performed comparing the highest (red) and lowest (blue) *FIP1L1* expressing patients. (B) Heatmap depicting significantly enriched gene ontology (GO) terms of upregulated genes in *FIP1L1* low-expressing patients and in Kasumi-1 cells upon *FIP1L1* knockdown. (C) Plots from GSEA of the RNA-sequencing analysis described in panel A. (D) Western blot showing *FIP1L1* and actin (loading control) protein in HL-60 and NB4 cells after transduction with control shRNAs or shRNAs targeting *FIP1L1* [shRNA (2) or (3)]. (E) Percentage of CD11b<sup>+</sup> HL-60 and NB4 cells, measured by flow cytometry, 5 days after transduction with shRNAs targeting *FIP1L1* or a control shRNA. Data are mean  $\pm$  standard deviation (SD) of 3

confirmed 3'UTR-APA-mediated regulation of BAALC expression, a negative prognostic factor in leukemia that blocks differentiation in both AML<sup>37</sup> and congenital neutropenia.<sup>72</sup> These APA events represent 2 of many that contributed to the differentiation phenotype observed.

We also observed dysregulation of leukemogenic pathways that hinder differentiation independent of AML1-ETO and BAALC. Specifically, targeting *FIP1L1* prompted downregulation of MYC, an oncogenic transcription factor well known for its role in blocking hematopoietic differentiation.<sup>73,74</sup> Although MYC protein was downregulated, MYC polyadenylation was unchanged (supplemental Figure 9B). Indirect MYC downregulation may be mediated by attenuated mTORC1 signaling, as activated mTOR promotes MYC translation.<sup>70,75</sup> Although we observed attenuation of activity, mTOR APA was also unchanged (supplemental Figure 9C). Furthermore, MYC indirectly regulates mTORC1 signaling by transcriptional control of cell membrane transporters that supply the amino acids required for mTORC1 activity.<sup>76-78</sup> Our data support this feedback loop as rapamycin signatures were linked to those for amino acid deprivation (supplemental Figure 9D). Although the details of this indirect APA mechanism are unclear, we show that targeting APA disrupts this oncogenic positive feedback loop and promotes leukemia cell differentiation (Figure 6F).

Our data also revealed that targeting a core APA machinery factor exhibits some degree of specificity (ie, transcripts were differentially shortened, lengthened, or unaffected upon *FIP1L1* knockdown). This finding agrees with previous reports of *FIP1L1* depletion in murine embryonic stem cells<sup>48</sup> and myoblasts.<sup>49</sup> *FIP1L1* is an RBP that binds to U-rich or AU-rich regions near the core polyadenylation cis-acting elements.<sup>48,79,80</sup> Therefore, *FIP1L1* may most prominently affect APA of transcripts that have putative binding motifs. Furthermore, binding can occur between the PAS hexamer and cleavage site<sup>79,80</sup> or upstream of the PAS hexamer.<sup>48,79</sup> The location of *FIP1L1* binding and distance between adjacent PAS hexamers have both been proposed to mediate differences in PAS usage patterns among transcripts.<sup>48,49</sup> Indeed, motif enrichment analysis based on our 3'READS data supports this idea that the location of *FIP1L1* binding relative to the PAS hexamer may mediate specificity. Upon *FIP1L1* knockdown, PAS usage with downstream A/U-rich regions was enhanced, whereas usage of sites with upstream A/U-rich regions was depleted (supplemental Figure 10). These data suggest that upstream binding of *FIP1L1* promotes, whereas downstream binding inhibits, PAS usage. Further work will be required to test this hypothesis. Finally, it is important to note that some of the transcripts with altered APA upon *FIP1L1* knockdown in our cellular system may not be direct *FIP1L1* targets and may be indirectly altered by changes in cellular behavior, such as decreased proliferation and/or increased differentiation.<sup>9</sup>

Altogether, our findings introduce APA as a putative target for differentiation therapy in AML. Historically, differentiation therapy by all-trans retinoic acid and arsenic trioxide has been most effective in patients with APL.<sup>81</sup> Recently, interest in differentiation therapy has been reinvigorated by the efficacy of IDH inhibitors in AML patients with *IDH1/2* mutations.<sup>27-29</sup> Our findings illuminate another possible target for differentiation therapy that may expand the number of patients who can benefit from differentiation-based treatment. Supporting the therapeutic potential of targeting APA regulators in leukemia, 2 recent reports have identified CPSF3 as the molecular target of JTE-607, a compound that is preferentially detrimental to leukemia cell lines.<sup>82,83</sup> CPSF3 is a member of the CPSF complex alongside *FIP1L1*, and treatment of AML cells with this CPSF3 inhibitor promotes differentiation and apoptosis. It will be exciting to test whether targeting additional polyadenylation regulators also promotes AML cell differentiation. Finally, to fully establish *FIP1L1* and other APA regulators as viable therapeutic targets, additional work is required to address the effect of targeting these regulators in healthy hematopoietic cells. Although we did not test the effect of *FIP1L1* knockdown on healthy cells, we noted that *FIP1L1* expression does not correlate with cell maturity in normal hematopoiesis as it does in patients with AML (supplemental Figure 7B).

The identification of *FIP1L1* in leukemogenesis is also clinically intriguing because it is a member of 2 oncofusions found in chronic eosinophilic leukemia and juvenile myelomonocytic leukemia/APL: *FIP1L1*-PDGFRA<sup>84</sup> and *FIP1L1*-RARA,<sup>85,86</sup> respectively. The reported contribution of *FIP1L1* in *FIP1L1*-RARA is limited to receptor dimerization and activation, with no data regarding the impact on global polyadenylation.<sup>87</sup> Similarly, reports regarding *FIP1L1*-PDGFRA describe *FIP1L1* as dispensable, claiming that constitutive activation of the receptor is sufficient to induce leukemia in cell lines and mouse models.<sup>88,89</sup> Despite this dismissal, not all signaling features dysregulated in chronic eosinophilic leukemia are recapitulated with only the C-terminal portion of PDGFRA.<sup>90</sup> In both fusions, *FIP1L1* retains the major protein-protein interaction domain but lacks the C-terminal domain implicated in RNA-binding.<sup>79</sup> Although our experiments do not directly address the role of *FIP1L1* RNA-binding in the observed phenotypes, our data support a likely consequence of *FIP1L1* alteration in these fusions and overall contribution to pathogenesis. Consequently, our findings necessitate further study regarding the impact of these 2 oncofusions on polyadenylation dysregulation in patients.

In conclusion, we have shown that APA dysregulation contributes to the differentiation block of AML, which can be overcome by downregulating the cleavage and polyadenylation factor *FIP1L1*. Consequently, targeting APA may be a promising therapeutic strategy for patients with leukemia.

**Figure 5 (continued)** independent experiments. \**P* < .05, \*\**P* < .01, \*\*\**P* < .001, 1-way analysis of variance (ANOVA) with a post hoc Tukey test. (F) Wright-Giemsa staining of HL-60 cell cytopspins, 5 days after transduction with shRNAs targeting *FIP1L1* or a control shRNA (400×). Irregular-shaped nuclei observed in sh*FIP1L1* image are indicative of granulocytic differentiation compared with the spherical, smooth-edged nuclei observed in the shControl image. (G) Proliferation of HL-60 and NB4 cells after transduction with shRNAs targeting *FIP1L1* or a control shRNA. Cells were seeded (day 0) after 2 days of puromycin selection. The graphs display the mean and SD of 3 technical replicates in 1 representative experiment of 2 independent experiments per cell line. \*\**P* < .01, \*\*\**P* < .001, multiple Student *t* tests using the Holm-Šidák method. (H) Percentage of Annexin V-positive apoptotic HL-60 and NB4 cells 4 days after transduction with shRNAs targeting *FIP1L1* or control shRNAs. Data are mean ± SD of 3 independent experiments. \**P* < .05, \*\**P* < .01, \*\*\**P* < .001, 1-way ANOVA with a post hoc Tukey test. FDR, false discovery rate; NES, normalized enrichment score.

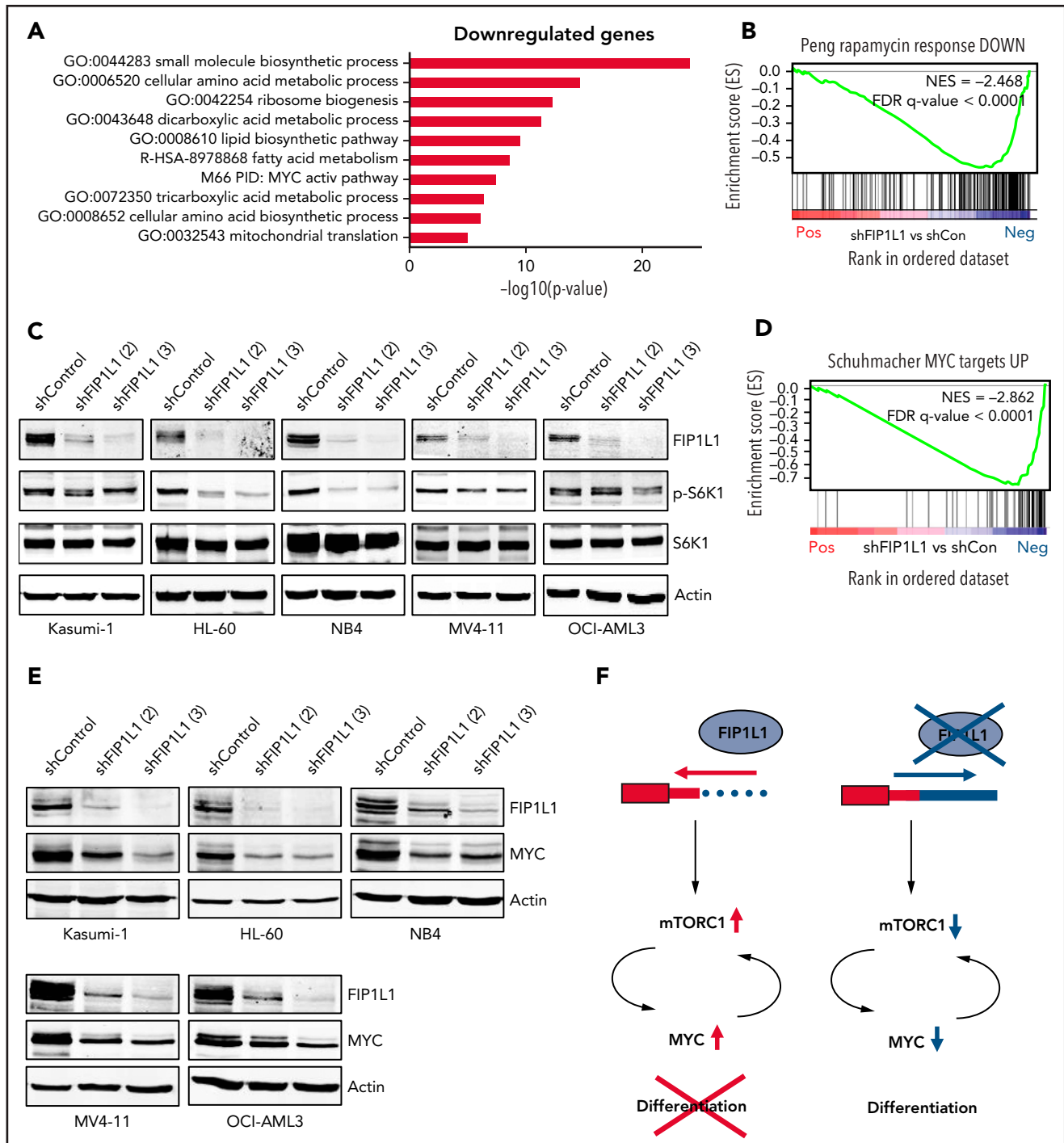


**Figure 6. Targeting APA converges on mTORC1 signaling and MYC expression.** (A) Metascape analysis of significantly downregulated genes ( $P < .01$ , 1.5× fold change) upon FIP1L1 knockdown in Kasumi-1 cells. (B) Plot from GSEA of the RNA-sequencing experiment presented in Figure 3A (supplemental Figure 5A-B) showing genes downregulated upon rapamycin treatment. (C) Western blot showing FIP1L1, phosphorylated p70-S6 Kinase 1 (p-S6K1), S6K1, and actin (loading control) protein in the indicated AML cell lines after transduction with control shRNAs or shRNAs targeting *FIP1L1* [shRNA (2) or (3)]. One representative experiment is shown of 2 independent experiments for each cell line. (D) Plot from GSEA of the RNA-sequencing experiment presented in Figure 3A (supplemental Figure 5A-B) showing genes upregulated by the oncogenic MYC transcription factor. (E) Western blot showing FIP1L1, MYC, and actin (loading control) protein in the indicated AML cell lines after transduction with control shRNAs or shRNAs targeting *FIP1L1*. One representative experiment is shown of 2 independent experiments for each cell line. (F) Cartoon model showing the impact of targeting APA on a positive oncogenic feedback loop. (Left) In cancer, mTORC1 and MYC positively regulate each other, blocking cellular differentiation. (Right) Targeting APA by FIP1L1 knockdown reduced both mTORC1 signaling and MYC transcriptional networks, promoting leukemia cell differentiation. Further work will elucidate the precise posttranscriptional targets responsible for disrupting this oncogenic signaling network. FDR, false discovery rate; NES, normalized enrichment score.



## Acknowledgments

The authors thank the staff at the UC San Diego Institute for Genomic Medicine for their help in sequencing both 3'READS and RNA-sequencing libraries. The authors also thank Qingbao Ding for his technical assistance.

This work was supported by the National Institutes of Health, National Cancer Institute (R01CA104509 [D.-E.Z.]) and the National Institute of General Medical Sciences (R01GM084089 [B.T.]). This work was also supported by a National Institutes of Health training grant (5T32GM007240-38 [A.G.D.]).

## Authorship

Contribution: A.G.D. and D.-E.Z. devised the study and designed the experimental strategies; A.G.D., D.T.J., and S.A.S. performed the research, collected data, and analyzed the results; D.Z. and J.S. prepared the 3'READS libraries; R.W. performed the bioinformatics analyses pertaining to the 3'READS experiments; N.D.J., M.L., and L.W. performed additional bioinformatics analyses of publicly available patient data sets; J.-H.Z. and E.D.B. collected, annotated, and provided clinical samples for the study; A.G.D. wrote the manuscript; D.T.J. edited the manuscript; B.T. provided resources, imparted expertise, and critically reviewed the manuscript; E.D.B. also critically reviewed the manuscript; and D.-E.Z. oversaw the study, supervised manuscript preparation, and secured funding to support the study.

Conflict-of-interest disclosure: The authors declare no competing financial interests.

ORCID profiles: A.G.D., 0000-0003-4356-7480; D.T.J., 0000-0003-4669-037X; D.Z., 0000-0002-4500-7666; R.W., 0000-0002-4211-5207; N.D.J., 0000-0003-4868-7182; M.L., 0000-0003-2057-723X; J.S., 0000-0001-6034-2027; L.W., 0000-0001-7825-0518; B.T., 0000-0001-8903-8256; D.-E.Z., 0000-0003-2541-6443.

Correspondence: Dong-Er Zhang, 9500 Gilman Dr #0815, La Jolla, CA 92037; e-mail: dez@ucsd.edu.

## Footnotes

Submitted 11 March 2020; accepted 16 August 2021; prepublished online on *Blood* First Edition 5 September 2021. DOI 10.1182/blood.2020005693.

The online version of this article contains a data supplement.

There is a *Blood* Commentary on this article in this issue.

The publication costs of this article were defrayed in part by page charge payment. Therefore, and solely to indicate this fact, this article is hereby marked "advertisement" in accordance with 18 USC section 1734.

## REFERENCES

- de Rooij LPMH, Chan DCH, Keyvani Chahi A, Hope KJ. Post-transcriptional regulation in hematopoiesis: RNA binding proteins take control. *Biochem Cell Biol*. 2019;97(1):10-20.
- Saez B, Walter MJ, Graubert TA. Splicing factor gene mutations in hematologic malignancies. *Blood*. 2017; 129(10):1260-1269.
- Zipeto MA, Court AC, Sadarangani A, et al. ADAR1 activation drives leukemia stem cell self-renewal by impairing let-7 biogenesis. *Cell Stem Cell*. 2016;19(2):177-191.
- Vu LP, Pickering BF, Cheng Y, et al. The N<sup>6</sup>-methyladenosine (m<sup>6</sup>A)-forming enzyme METTL3 controls myeloid differentiation of normal hematopoietic and leukemia cells. *Nat Med*. 2017;23(11):1369-1376.
- Guo S, Lu J, Schlanger R, et al. MicroRNA miR-125a controls hematopoietic stem cell number. *Proc Natl Acad Sci U S A*. 2010; 107(32):14229-14234.
- Alt FW, Bothwell AL, Knapp M, et al. Synthesis of secreted and membrane-bound immunoglobulin mu heavy chains is directed by mRNAs that differ at their 3' ends. *Cell*. 1980;20(2):293-301.
- Takagaki Y, Seipelt RL, Peterson ML, Manley JL. The polyadenylation factor CstF-64 regulates alternative processing of IgM heavy chain pre-mRNA during B cell differentiation. *Cell*. 1996;87(5):941-952.
- Chuvpilo S, Zimmer M, Kerstan A, et al. Alternative polyadenylation events contribute to the induction of NF-ATc in effector T cells. *Immunity*. 1999;10(2): 261-269.
- Sandberg R, Neilson JR, Sarma A, Sharp PA, Burge CB. Proliferating cells express mRNAs with shortened 3' untranslated regions and fewer microRNA target sites. *Science*. 2008; 320(5883):1643-1647.
- Singh I, Lee SH, Sperling AS, et al. Widespread intronic polyadenylation diversifies immune cell transcriptomes. *Nat Commun*. 2018;9(1):1716.
- Lee SH, Singh I, Tisdale S, Abdel-Wahab O, Leslie CS, Mayr C. Widespread intronic polyadenylation inactivates tumour suppressor genes in leukaemia. *Nature*. 2018;561(7721):127-131.
- Lee SH, Mayr C. Gain of additional BIRC3 protein functions through 3'-UTR-mediated protein complex formation. *Mol Cell*. 2019; 74(4):701-712.e9.
- Tian B, Hu J, Zhang H, Lutz CS. A large-scale analysis of mRNA polyadenylation of human and mouse genes. *Nucleic Acids Res*. 2005;33(1):201-212.
- Mayr C, Bartel DP. Widespread shortening of 3'UTRs by alternative cleavage and polyadenylation activates oncogenes in cancer cells. *Cell*. 2009;138(4):673-684.
- Berkovits BD, Mayr C. Alternative 3' UTRs act as scaffolds to regulate membrane protein localization. *Nature*. 2015; 522(7556):363-367.
- Miles WO, Lembo A, Volorio A, et al. Alternative polyadenylation in triple-negative breast tumors allows NRAS and c-JUN to bypass PUMILIO posttranscriptional regulation. *Cancer Res*. 2016;76(24):7231-7241.
- Ji Z, Lee JY, Pan Z, Jiang B, Tian B. Progressive lengthening of 3' untranslated regions of mRNAs by alternative polyadenylation during mouse embryonic development. *Proc Natl Acad Sci U S A*. 2009;106(17):7028-7033.
- Hilgers V, Perry MW, Hendrix D, Stark A, Levine M, Haley B. Neural-specific elongation of 3' UTRs during *Drosophila* development. *Proc Natl Acad Sci U S A*. 2011;108(38):15864-15869.
- Ulitsky I, Shkumatava A, Jan CH, et al. Extensive alternative polyadenylation during zebrafish development. *Genome Res*. 2012; 22(10):2054-2066.
- Elkon R, Drost J, van Haaften G, et al. E2F mediates enhanced alternative polyadenylation in proliferation. *Genome Biol*. 2012;13(7):R59.
- Masamha CP, Xia Z, Yang J, et al. CFIm25 links alternative polyadenylation to glioblastoma tumour suppression. *Nature*. 2014;510(7505):412-416.
- Xia Z, Donehower LA, Cooper TA, et al. Dynamic analyses of alternative polyadenylation from RNA-seq reveal a 3'-UTR landscape across seven tumour types. *Nat Commun*. 2014;5(1):5274.
- Akman HB, Oyken M, Tuncer T, Can T, Erson-Bensan AE. 3'UTR shortening and EGF signaling: implications for breast cancer. *Hum Mol Genet*. 2015; 24(24):6910-6920.
- Tenen DG. Disruption of differentiation in human cancer: AML shows the way. *Nat Rev Cancer*. 2003;3(2):89-101.
- Huang ME, Ye YC, Chen SR, et al. Use of all-trans retinoic acid in the treatment of acute promyelocytic leukemia. *Blood*. 1988; 72(2):567-572.
- Niu C, Yan H, Yu T, et al. Studies on treatment of acute promyelocytic leukemia with arsenic trioxide: remission induction, follow-up, and molecular monitoring in 11 newly diagnosed and 47 relapsed acute



- promyelocytic leukemia patients. *Blood*. 1999;94(10):3315-3324.
27. Wang F, Travins J, DeLaBarre B, et al. Targeted inhibition of mutant IDH2 in leukemia cells induces cellular differentiation. *Science*. 2013; 340(6132):622-626.
28. Golub D, Iyengar N, Dogra S, et al. Mutant isocitrate dehydrogenase inhibitors as targeted cancer therapeutics. *Front Oncol*. 2019;9:417.
29. Mugoni V, Panella R, Cheloni G, et al. Vulnerabilities in mIDH2 AML confer sensitivity to APL-like targeted combination therapy. *Cell Res*. 2019;29(6):446-459.
30. Hoque M, Ji Z, Zheng D, et al. Analysis of alternative cleavage and polyadenylation by 3' region extraction and deep sequencing. *Nat Methods*. 2013;10(2):133-139.
31. Zheng D, Liu X, Tian B. 3'READS+, a sensitive and accurate method for 3' end sequencing of polyadenylated RNA. *RNA*. 2016;22(10):1631-1639.
32. Gupta I, Clauder-Münster S, Klaus B, et al. Alternative polyadenylation diversifies post-transcriptional regulation by selective RNA-protein interactions. *Mol Syst Biol*. 2014; 10(2):719.
33. Akman BH, Can T, Erson-Bensan AE. Estrogen-induced upregulation and 3'-UTR shortening of CDC6. *Nucleic Acids Res*. 2012;40(21):10679-10688.
34. Langer C, Radmacher MD, Ruppert AS, et al; Cancer and Leukemia Group B (CALGB). High BAALC expression associates with other molecular prognostic markers, poor outcome, and a distinct gene-expression signature in cytogenetically normal patients younger than 60 years with acute myeloid leukemia: a Cancer and Leukemia Group B (CALGB) study. *Blood*. 2008; 111(11):5371-5379.
35. Damiani D, Tiribelli M, Franzoni A, et al. BAALC overexpression retains its negative prognostic role across all cytogenetic risk groups in acute myeloid leukemia patients. *Am J Hematol*. 2013;88(10):848-852.
36. Heuser M, Berg T, Kuchenbauer F, et al. Functional role of BAALC in leukemogenesis. *Leukemia*. 2012; 26(3):532-536.
37. Morita K, Masamoto Y, Kataoka K, et al. BAALC potentiates oncogenic ERK pathway through interactions with MEKK1 and KLF4. *Leukemia*. 2015;29(11):2248-2256.
38. Ray D, Kwon SY, Tagoh H, Heidenreich O, Ptasinska A, Bonifer C. Lineage-inappropriate PAX5 expression in t(8;21) acute myeloid leukemia requires signaling-mediated abrogation of polycomb repression. *Blood*. 2013;122(5):759-769.
39. Spies N, Burge CB, Bartel DP. 3' UTR-isoform choice has limited influence on the stability and translational efficiency of most mRNAs in mouse fibroblasts. *Genome Res*. 2013;23(12):2078-2090.
40. Gruber AR, Martin G, Müller P, et al. Global 3' UTR shortening has a limited effect on protein abundance in proliferating T cells. *Nat Commun*. 2014;5(1):5465.
41. Kaida D, Berg MG, Younis I, et al. U1 snRNP protects pre-mRNAs from premature cleavage and polyadenylation. *Nature*. 2010; 468(7324):664-668.
42. Li B, Yang FC, Clapp DW, Chun KT. Enforced expression of CUL-4A interferes with granulocytic differentiation and exit from the cell cycle. *Blood*. 2003; 101(5):1769-1776.
43. Li B, Jia N, Kapur R, Chun KT. Cul4A targets p27 for degradation and regulates proliferation, cell cycle exit, and differentiation during erythropoiesis. *Blood*. 2006;107(11):4291-4299.
44. Seipel K, Messerli C, Wiedemann G, Bacher U, Pabst T. MN1, FOXP1 and hsa-miR-181a-5p as prognostic markers in acute myeloid leukemia patients treated with intensive induction chemotherapy and autologous stem cell transplantation. *Leuk Res*. 2020; 89:106296.
45. Naudin C, Hattabi A, Michelet F, et al. PUMILIO/FOXP1 signaling drives expansion of hematopoietic stem/progenitor and leukemia cells. *Blood*. 2017; 129(18):2493-2506.
46. Gascoyne DM, Banham AH. The significance of FOXP1 in diffuse large B-cell lymphoma. *Leuk Lymphoma*. 2017;58(5):1037-1051.
47. Lin Y, Li Z, Oszolak F, et al. An in-depth map of polyadenylation sites in cancer. *Nucleic Acids Res*. 2012;40(17):8460-8471.
48. Lackford B, Yao C, Charles GM, et al. Fip1 regulates mRNA alternative polyadenylation to promote stem cell self-renewal. *EMBO J*. 2014;33(8):878-889.
49. Li W, You B, Hoque M, et al. Systematic profiling of poly(A)<sup>+</sup> transcripts modulated by core 3' end processing and splicing factors reveals regulatory rules of alternative cleavage and polyadenylation. *PLoS Genet*. 2015;11(4):e1005166.
50. Gupta D, Shah HP, Malu K, Berliner N, Gaines P. Differentiation and characterization of myeloid cells. *Curr Protoc Immunol*. 2014;104:22F.5.1-22F.5.28.
51. Draber P, Stepanek O, Hrdinka M, et al. LST1/A is a myeloid leukocyte-specific transmembrane adaptor protein recruiting protein tyrosine phosphatases SHP-1 and SHP-2 to the plasma membrane. *J Biol Chem*. 2012;287(27):22812-22821.
52. Raffel S, Falcone M, Kneisel N, et al. BCAT1 restricts αKG levels in AML stem cells leading to IDHmut-like DNA hypermethylation [published correction appears in *Nature*. 2018;560(7718):E28]. *Nature*. 2017; 551(7680):384-388.
53. Gu Z, Liu Y, Cai F, et al. Loss of EZH2 reprograms BCAA metabolism to drive leukemic transformation. *Cancer Discov*. 2019;9(9):1228-1247.
54. Somerville TC, Matheny CJ, Spencer GJ, et al. Hierarchical maintenance of MLL myeloid leukemia stem cells employs a transcriptional program shared with embryonic rather than adult stem cells. *Cell Stem Cell*. 2009;4(2):129-140.
55. Burel SA, Harakawa N, Zhou L, Pabst T, Tenen DG, Zhang DE. Dichotomy of AML1-ETO functions: growth arrest versus block of differentiation. *Mol Cell Biol*. 2001; 21(16):5577-5590.
56. de Guzman CG, Warren AJ, Zhang Z, et al. Hematopoietic stem cell expansion and distinct myeloid developmental abnormalities in a murine model of the AML1-ETO translocation. *Mol Cell Biol*. 2002;22(15):5506-5517.
57. Dunne J, Cullmann C, Ritter M, et al. siRNA-mediated AML1/MTG8 depletion affects differentiation and proliferation-associated gene expression in t(8;21)-positive cell lines and primary AML blasts. *Oncogene*. 2006;25(45):6067-6078.
58. Heidenreich O, Krauter J, Riehle H, et al. AML1/MTG8 oncogene suppression by small interfering RNAs supports myeloid differentiation of t(8;21)-positive leukemic cells. *Blood*. 2003;101(8):3157-3163.
59. Tonks A, Tonks AJ, Pearn L, et al. Expression of AML1-ETO in human myelomonocytic cells selectively inhibits granulocytic differentiation and promotes their self-renewal. *Leukemia*. 2004;18(7):1238-1245.
60. Zaidi SK, Perez AW, White ES, Lian JB, Stein JL, Stein GS. An AML1-ETO/miR-29b-1 regulatory circuit modulates phenotypic properties of acute myeloid leukemia cells. *Oncotarget*. 2017;8(25):39994-40005.
61. Fu L, Shi J, Liu A, et al. A microcircuitry of microRNA-9-1 and RUNX1-RUNX1T1 contributes to leukemogenesis in t(8;21) acute myeloid leukemia. *Int J Cancer*. 2017; 140(3):653-661.
62. Johnson DT, Davis AG, Zhou JH, Ball ED, Zhang DE. MicroRNA let-7b downregulates AML1-ETO oncogene expression in t(8;21) AML by targeting its 3'UTR. *Exp Hematol Oncol*. 2021;10(1):8.
63. Ley TJ, Miller C, Ding L, et al; Cancer Genome Atlas Research Network. Genomic and epigenomic landscapes of adult de novo acute myeloid leukemia. *N Engl J Med*. 2013;368(22):2059-2074.
64. Tyner JW, Tognon CE, Bottomly D, et al. Functional genomic landscape of acute myeloid leukaemia. *Nature*. 2018; 562(7728):526-531.
65. Yilmaz OH, Valdez R, Theisen BK, et al. Pten dependence distinguishes haematopoietic stem cells from leukaemia-initiating cells. *Nature*. 2006;441(7092):475-482.
66. Hoshii T, Tadokoro Y, Naka K, et al. mTORC1 is essential for leukemia propagation but not stem cell self-renewal. *J Clin Invest*. 2012;122(6):2114-2129.
67. Martelli AM, Evangelisti C, Chiarini F, McCubrey JA. The phosphatidylinositol 3-kinase/Akt/mTOR signaling network as a therapeutic target in acute myelogenous leukemia patients. *Oncotarget*. 2010; 1(2):89-103.

68. Choo AY, Yoon SO, Kim SG, Roux PP, Blenis J. Rapamycin differentially inhibits S6Ks and 4E-BP1 to mediate cell-type-specific repression of mRNA translation. *Proc Natl Acad Sci U S A*. 2008;105(45):17414-17419.
69. Jiang YP, Ballou LM, Lin RZ. Rapamycin-insensitive regulation of 4e-BP1 in regenerating rat liver. *J Biol Chem*. 2001; 276(14):10943-10951.
70. Wall M, Poortinga G, Hannan KM, Pearson RB, Hannan RD, McArthur GA. Translational control of c-MYC by rapamycin promotes terminal myeloid differentiation. *Blood*. 2008;112(6):2305-2317.
71. Wiestner A, Tehrani M, Chiorazzi M, et al. Point mutations and genomic deletions in CCND1 create stable truncated cyclin D1 mRNAs that are associated with increased proliferation rate and shorter survival. *Blood*. 2007;109(11):4599-4606.
72. Dannenmann B, Klimiankou M, Solovyeva A, et al. BAALC is a key mediator of leukemia development in congenital neutropenia. *Blood*. 2017;130(suppl 1):541.
73. Leon J, Ferrandiz N, Acosta JC, Delgado MD. Inhibition of cell differentiation: a critical mechanism for MYC-mediated carcinogenesis? *Cell Cycle*. 2009;8(8):1148-1157.
74. Delgado MD, León J. Myc roles in hematopoiesis and leukemia. *Genes Cancer*. 2010;1(6):605-616.
75. Gera JF, Mellinshoff IK, Shi Y, et al. AKT activity determines sensitivity to mammalian target of rapamycin (mTOR) inhibitors by regulating cyclin D1 and c-myc expression. *J Biol Chem*. 2004;279(4):2737-2746.
76. Yue M, Jiang J, Gao P, Liu H, Qing G. Oncogenic MYC activates a feedforward regulatory loop promoting essential amino acid metabolism and tumorigenesis. *Cell Rep*. 2017;21(13):3819-3832.
77. Liu P, Ge M, Hu J, et al. A functional mammalian target of rapamycin complex 1 signaling is indispensable for c-Myc-driven hepatocarcinogenesis. *Hepatology*. 2017; 66(1):167-181.
78. Zhao X, Petrashen AP, Sanders JA, Peterson AL, Sedivy JM. SLC1A5 glutamine transporter is a target of MYC and mediates reduced mTORC1 signaling and increased fatty acid oxidation in long-lived Myc hypomorphic mice. *Aging Cell*. 2019; 18(3):e12947.
79. Kaufmann I, Martin G, Friedlein A, Langen H, Keller W. Human Fip1 is a subunit of CPSF that binds to U-rich RNA elements and stimulates poly(A) polymerase. *EMBO J*. 2004;23(3):616-626.
80. Martin G, Gruber AR, Keller W, Zavolan M. Genome-wide analysis of pre-mRNA 3' end processing reveals a decisive role of human cleavage factor I in the regulation of 3' UTR length. *Cell Rep*. 2012;1(6):753-763.
81. Nowak D, Stewart D, Koeffler HP. Differentiation therapy of leukemia: 3 decades of development. *Blood*. 2009; 113(16):3655-3665.
82. Kakegawa J, Sakane N, Suzuki K, Yoshida T. JTE-607, a multiple cytokine production inhibitor, targets CPSF3 and inhibits pre-mRNA processing. *Biochem Biophys Res Commun*. 2019;518(1):32-37.
83. Ross NT, Lohmann F, Carbonneau S, et al. CPSF3-dependent pre-mRNA processing as a druggable node in AML and Ewing's sarcoma [published correction appears in *Nat Chem Biol*. 2020;16(4):479]. *Nat Chem Biol*. 2020;16(1):50-59.
84. Cools J, DeAngelo DJ, Gotlib J, et al. A tyrosine kinase created by fusion of the PDGFRA and FIP1L1 genes as a therapeutic target of imatinib in idiopathic hypereosinophilic syndrome. *N Engl J Med*. 2003;348(13):1201-1214.
85. Buijs A, Bruin M. Fusion of FIP1L1 and RARA as a result of a novel t(4;17)(q12;q21) in a case of juvenile myelomonocytic leukemia. *Leukemia*. 2007;21(5):1104-1108.
86. Kondo T, Mori A, Darmanin S, Hashino S, Tanaka J, Asaka M. The seventh pathogenic fusion gene FIP1L1-RARA was isolated from a t(4;17)-positive acute promyelocytic leukemia. *Haematologica*. 2008;93(9):1414-1416.
87. Iwasaki J, Kondo T, Darmanin S, et al. FIP1L1 presence in FIP1L1-RARA or FIP1L1-PDGFRα differentially contributes to the pathogenesis of distinct types of leukemia. *Ann Hematol*. 2014;93(9): 1473-1481.
88. Stover EH, Chen J, Folens C, et al. Activation of FIP1L1-PDGFRα requires disruption of the juxtamembrane domain of PDGFRα and is FIP1L1-independent. *Proc Natl Acad Sci U S A*. 2006;103(21): 8078-8083.
89. Vanden Bempt M, Demeyer S, Mentens N, et al. Generation of the Fip1l1-Pdgfra fusion gene using CRISPR/Cas genome editing. *Leukemia*. 2016; 30(9):1913-1916.
90. Buitenhuis M, Verhagen LP, Cools J, Coffey PJ. Molecular mechanisms underlying FIP1L1-PDGFRα-mediated myeloproliferation. *Cancer Res*. 2007;67(8):3759-3766.